

Original research

Purification of drinking water from dissolved Bisphenol-A (BPA) using zinc oxide nanoparticles

Safaa El-Nahas^{*1}, Mohammed Ezzeldien², Asmaa S. Ali¹

¹ Chemistry Department, Faculty of Science, South Valley University, Qena 83523, Egypt

² Metallurgy & Material Science Tests (MMST) Lab, Department of Physics, Faculty of Science, South Valley University, Qena, Egypt

Received: 16/11/2022

Accepted: 8/12/2022

© Unit of Environmental Studies and Development, Aswan University

Abstract:

The goal of this research is to study the potential of ZnO nanoparticles as an alternative material for the removal of bisphenol A (BPA) that can be used in ceramic membrane. This research has been studied various factors for the removal of BPA, including contact time, pH, temperature, initial BPA levels, and ZnO NPs dosage. The removal of BPA onto ZnO NPs matched well with the Langmuir, Freundlich, and Temkin isotherm models. The maximum removal efficiency under optimum conditions achieved 85%. The kinetic data fitted well the pseudo-second order model than other models. The phenomenon for removal of BPA was a spontaneous process and showed the endothermic nature. Thermodynamic, kinetics and isotherm data indicate that more than one mechanism was applied for removal of BPA from water.

Keywords: Bisphenol A, ZnO NPs, Ceramic membrane.

1- Introduction

Climate change has already had an impact on water supply and quality, and these effects are likely to persist as temperatures rise, precipitation patterns alter, and runoff rises. It can result in a lack of water. The industrial development generated large amounts of pollutants, most of them considered dangerous to human health (Manisalidis et al., 2020). Pollutants can be easily divided into four groups: chemical, physical, physiological, and biological. In general, there are two types of chemical contaminants: inorganic and organic (Englande et al., 2015). Phenolic and polyphenolic compounds are belonging to organic compounds and widely distributed in the environment, including wastewater and physical environmental water (Mainali, 2020). The US Environmental Protection Agency has considered phenolic compounds as harmful substances (Sun et al., 2014). Plastics had various commercial and industrial applications for their unique physical and chemical properties. Plastic use has a lot of harmful environmental repercussions as a result of inadequate waste management techniques (Evode et al., 2021). The IUPAC name of BPA is 2,2-bis(4-hydroxyphenyl) propane which was manufactured by the reaction of acetone and phenol. BPA has an estrogenic effect on human health and harms the aquatic environment.

Corresponding author*: E-mail address: safaa33@yahoo.com

Human exposure to BPA has increased through usage of materials produced of epoxy resins and polycarbonate plastics (Kang et al., 2006). The BPA materials are used as a monomer in the synthesis of polycarbonate plastic and epoxy resins which found inside food and beverage containers as well as water bottles and newborn milk bottles (HoekstraSimoneau, 2013). Diabetes, cardiovascular disease, and altered liver enzymes are among the health issues that have been linked to higher BPA exposure levels. Furthermore, elevated BPA levels were increased in the number of premature births and recurrent miscarriages in women. Also, BPA levels in men have been linked to the decreasing sperm quality and sperm DNA damage. The exposure to BPA during pregnancy may be linked to the increase in aggression and hyperactivity in children, especially in females (Rubin, 2011). The residual BPA left in polycarbonate after manufacture can diffuse into liquid foods, and the polymer can also hydrolyze when it comes into contact with water or watery foods. Nowadays, many people have concerned about the leakage of BPA from bottles under unfavorable conditions (hot temperatures and sunshine). Plastics with number codes no. 3 or 7 contain BPA molecules. Sometimes, type 7 plastics is substituted by the letters "PC" next to the recycling symbol (Elobeid et al., 2012). Techniques for eliminating BPA from aquatic habitats must be developed due to its negative impacts. These methods include ozonation, nano-filtration, reverse osmosis, photocatalytic breakdown, electrochemical oxidation, and biological processes. However, these methods have drawbacks, including sluggish reaction times, large driving forces, difficult operations, restricted applicability, and ineffective removal efficiency (Barzegari et al., 2015). BPA removal is preferred over adsorption because of its effectiveness, low operating costs, excellent selectivity, and ease of usage. Furthermore, the chosen adsorbent must be easily accessible, affordable, regenerable, and possess good selectivity for the intended pollutants (Siddiqi et al., 2018). The most widely utilized nanoparticles for water treatment include silica, titanium oxide, copper oxide, zinc oxide, and zinc sulphide (Wang, J.Zhang, 2020). There has been a lot of interest in developing preparation techniques that enable the fabrication of ZnO nanostructures with precisely regulated size and form. (Yıldırım Durucan, 2010). ZnO NS was produced using a variety of techniques, such as sol-gel, biosynthetic, hydrothermal, electrochemical deposition, microwave, mechanical milling, sonochemical routes, chemical vapor deposition, and laser ablation (El-Nahas et al., 2021). Microwave processing provides a number of advantages, such as rapid heating, high repeatability, high purity, high yield, regulating size, quick crystallization, and organization of shape or morphology in nanostructures. Furthermore, it is a straightforward process that doesn't have any problems with temperature gradients (Monika Gaba 2010). ZnO can be employed in polymeric and ceramic membrane construction because of their performance in water and wastewater treatment applications (Sheikh et al., 2020). The purpose of this paper was to examine the efficiency of zinc oxide nanoparticles which may be used in ceramic membrane for removing bisphenol A from water.

2- Materials and Methods

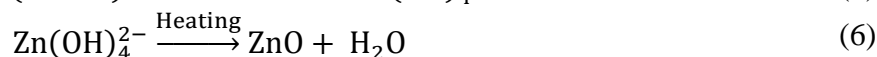
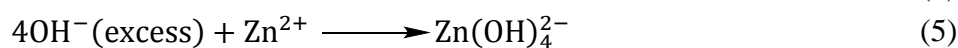
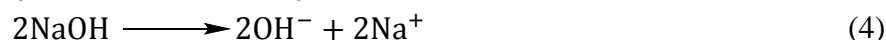
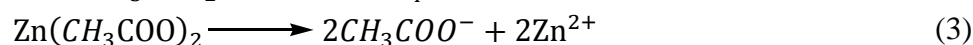
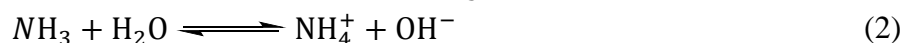
2.1 Chemicals and reagents

For the synthesis of ZnO NPs, $(\text{Zn}(\text{CH}_3\text{COO})_2 \cdot 2\text{H}_2\text{O})$ of purity over 99% and hexamethylenetetramine (HMTA, $\text{C}_6\text{H}_{12}\text{N}_4$, purity $\geq 99\%$) were purchased from Merck Co. (Germany). Bis phenol A (BPA) (purity over 97%) was supplied from Alfa Aesar Co. (Germany). Different working BPA solutions with the required concentrations were prepared by diluting the stock solution (10 mg/l). All other chemicals are analytical grade and used as

received without moreover purification. (0.01M HCl) and (0.01M NaOH) solutions were used to adjust the pH of the solutions.

2.2 Synthesis of ZnO NPs

Based on the methodology described (El-Nahas et al., 2021) and the written equations (1-6), briefly: an aqueous equimolar of (0.15 M) HMTA was added drop wisely to (0.15 M) zinc acetate dihydrate at room temperature, then the solution was agitated for 1 hour to keep the pH at 6.7. The resulted solution was subjected to microwave irradiation for 15 minutes using a domestic microwave system (a Daewoo microwave oven) at power 200 Watt followed by 10 minutes. Finally, the white precipitate was separated through centrifugation at 6000 rpm for 10 min followed by rinsing with deionized water and 70% ethanol several times and dried at 80°C overnight. The solid sample was calcined at 500°C for 3 hrs in a muffle furnace as elucidated from TGA results. The oxide was stored in brown sealed bottles under dry conditions until use.



2.3 Instruments

FTIR spectra were Shimadzu FTIR, Kyoto, Japan - . A scanning electron microscope (SEM, JSM-5500LV type - EDAX; Inspect S 50, FEI, Netherlands- A shaker model (WB-110X) with temperature control- UV- visible (PG Instruments UV, model T80, UK - HACH precision pH-meter (Model Sension7 -Powder X-ray Diffraction Analysis (XRD) Bruker Axs-D8 at 2θ range between 10→-90→.

2.4 Adsorption experiments

The studied ZnO NPs sample's capacity for adsorbing the BPA was evaluated in batch mode. This is due to its simplicity, consistency, and ease of extrapolation to a larger scale for a practical application (El-Nahas et al., 2017).The adsorption factors were investigated at initial concentration (1 - 5 ppm), pH (4 - 10), contact time (15 - 90 min), Adsorbent dosage (0.1 – 2 g /L) and operating temperature (25- 55 °C). At various times, a known volume (1 g/L) of sorbent containing 100 ml of a BPA solution containing 1 mg/L of ZnO NPs was stirred at 150 rpm in capped glass bottles (250 ml). After the samples were filtered off, the residual BPA concentration in the supernatant was measured using a spectrophotometer in accordance with the direct photometric method (Baird et al., 2017). Equation 7 and 8 were used to determine the percentage removal efficiency and amount of BPA adsorbed (q_e) (El-Nahas et al., 2020).

$$\% \text{ Removal of BPA} = \frac{C_0 - C_e}{C_0} \times 100 \quad (7)$$

$$q_e = \frac{C_0 - C_e}{m} \times \frac{V}{1000} \quad (8)$$

Where, the C_0 and C_e are the initial BPA concentration and the final BPA concentration at equilibrium (mg/L), m is the mass of adsorbent dose (g), V is the volume of the solution (ml).

2.5 Determination the Point of Zero Charge (PZC)

The pH value is zero for ZnO NPs is measured when all positive and negative charges at the surface of adsorbent were equal. Five bottles containing 100 ml of NaCl (0.01M) and 0.1 g of sorbent were used to evaluate the point of zero charge (PZC) for ZnO NPs material. The pH of each bottle's starting solution was altered by simultaneously adding either 0.5 M NaOH or 0.5 M HCl solutions. The final pH (pH_f) of the solutions was measured after 48 hours of agitation with the sorbent, ΔpH was calculated ($\Delta pH = pH_i - pH_f$) and plotted versus pH_i . The PZC will be the point which reaches the null value variation (at $\Delta pH = 0$) (El-Nahas. et al., 2017).

3. RESULTS AND DISCUSSION

3.1 Characterizations of the ZnO NPs

3.1.1 Fourier transform infrared (FT-IR) analysis

Infrared radiation in Fourier transform infrared spectroscopy (FTIR) technique is a good method for identifying the functional groups in compounds. This technique displayed certain functional groups on the surface of ZnO NPs responsible for BPA elimination. FTIR spectroscopy diagram was illustrated in the 400–4000 cm^{-1} region (Figure 1). The results demonstrated a wide band at 3454 cm^{-1} where may be attributed to water molecules adsorbed on the surface of ZnO NPs. Another distinctive Zn-O band was detected at 445 cm^{-1} as a result of symmetric bending vibration of ZnO NPs (El-Nahas et al., 2021; Soliman et al., 2020).

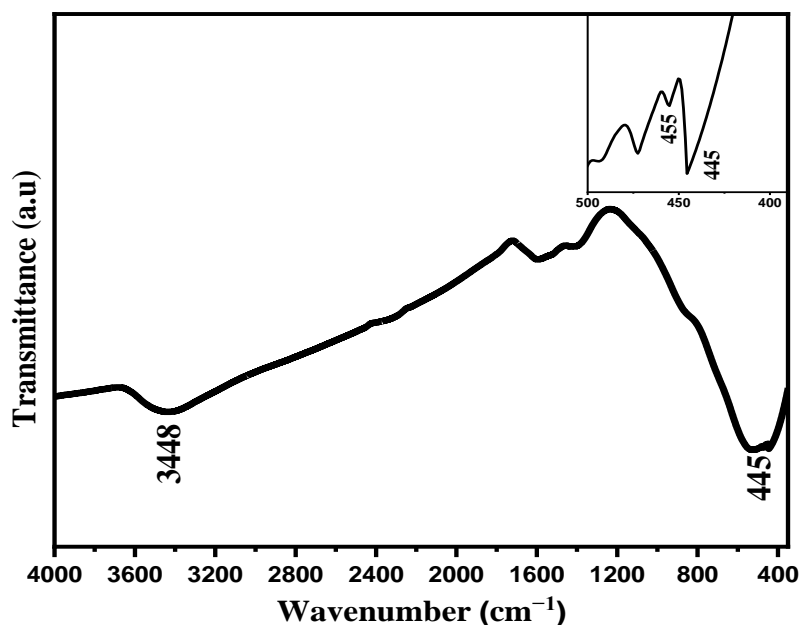


Figure 1: FTIR of ZnO NPs sample.

3.1.2 XRD analysis

X-ray powder diffraction (XRD) is a flexible, non-destructive analytical technique for the characterization and analytical evaluation of crystalline phases present in powdered and bulk materials. Every phase or mineral, there may be a distinct diffraction pattern that depends on the

crystal structure, chemical structure, crystallite size, and lattice strain of the material (Bezzon et al., 2022). The structured ZnO NPs was detected as Wurtzite phase (JCPDS: No.01-075-0576). The great intensity of diffraction peaks demonstrated (Figure 2) the high crystallinity of ZnO NPs sample. The 2θ angles of ZnO NPs were 31.77° , 34.43° , 36.3° , 47.5° , 56.6° , 67.9° , 72.6° , and 76.9° which had indexes (1 0 0), (1 0 1), (1 0 2), (2 1 0), (1 0 3), (2 1 2), (0 0 4), and (2 0 2) planes, respectively. The data in Table 1 derived from XRD pattern exhibited that the good crystallinity of ZnO NPs and have specific surface area (SSA) of $44.38 \text{ m}^2\text{g}^{-1}$ (calculated by equation 9). The particle size (D) was calculated by Scherrer method (equation 10) was 24.10 nm which indicating the sample was in nanoscale (El-Nahas et al., 2021).

$$\text{SSA} = \frac{6 \times 10^3}{D_p \times \rho} (\text{m}^2 \text{g}^{-1}) \quad (9)$$

$$D = \frac{k\lambda}{\beta_{hkl} \cos\theta} \quad (10)$$

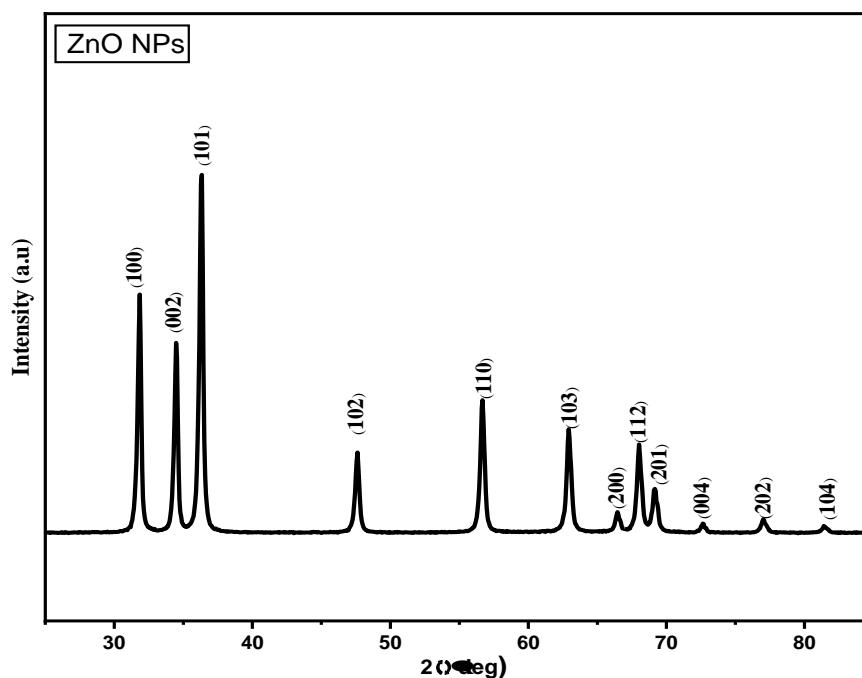


Figure 2: XRD of ZnO NPs sample

Table 1: Lattice parameters phases and surface area of ZnO NPs

Sample	Lattice constants			$V(\text{nm})^3$ Unit cell	D (nm) Scherrer	SSA (m^2g^{-1})	phase
	A	b	c/a				
ZnO NPs	3.258	5.22	1.6018	48.009	24.10	44.38	Wurtzite

3.1.3 SEM and EDX analyses

Scanning electron microscope (SEM) gives magnified images and reveal some microscopic-scale information as size, shape, composition, crystallography, and other physical

and chemical features of a material (Rezaeizadeh et al., 2021). The SEM image of the ZnO NPs sample have short rod-like structure as shown in Figure 3. Other researchers showed the same SEM structure by some of preparation methods (Hasanpoor et al., 2015). The morphology of ZnO can be altered as needle-shaped or flower-shaped particles utilizing the microwave (El-Nahas, et al., 2021;Jun , 2002). EDX spectroscopy is used to identify the composition of elements that make up a sample (Abd Mutalib et al., 2017; Scimeca et al., 2018). According to the EDX spectrum of ZnO nanoparticles in Figure 4 the prepared sample (ZnO NPs) contains only zinc and oxygen without contaminants (Table 2). The high-intensity peaks for zinc and oxygen indicate the good crystallinity of the sample (Singh et al., 2012).

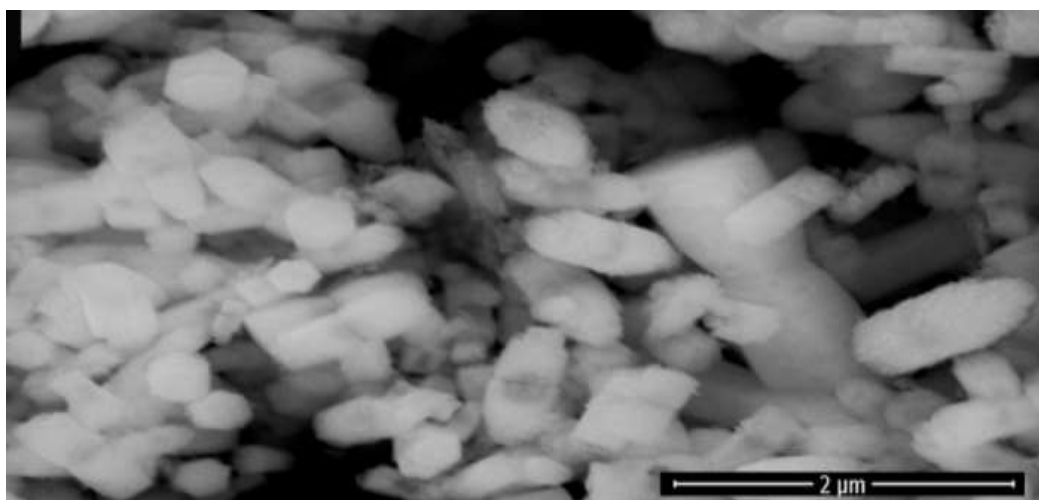


Figure 3: SEM analysis of ZnO NPs sample

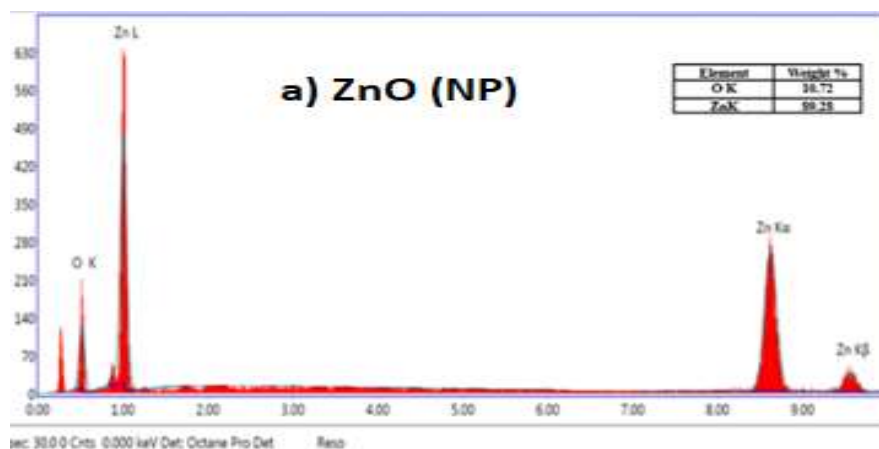


Figure 4: EDX analysis of ZnO NPs samples.

3.2 Study of Point of Zero Charge (PZC)

It is necessary to determine the sample's acidity or basicity and identifying the surface's attractions for the tested ionic species which can be occurred by studying the point of zero charge (PZC). A point of zero charge (PZC) is a pH value where no charge on the surface (Divband Hafshejani et al., 2016). Figure 5 depicts the pH-related to adsorption of BPA onto

ZnO NPs. At pH levels below its PZC value (pH=7.3), the surface of ZnO NPs gains a net positive charge by the adsorption of extra H⁺ ions from the solution. Whereas at pH levels above its PZC value (>pH=7.3), the surface of ZnO NPs deprotonates H⁺ ions and gains a net negative charge. Similar trend were reported by other researchers (Godwin et al., 2022; ParkRegalbuto, 1995).

Table 2: EDX analysis for ZnO NPs sample.

Samples	Elemental Analysis	
	C	O
ZnO NPs	89.28	10.72

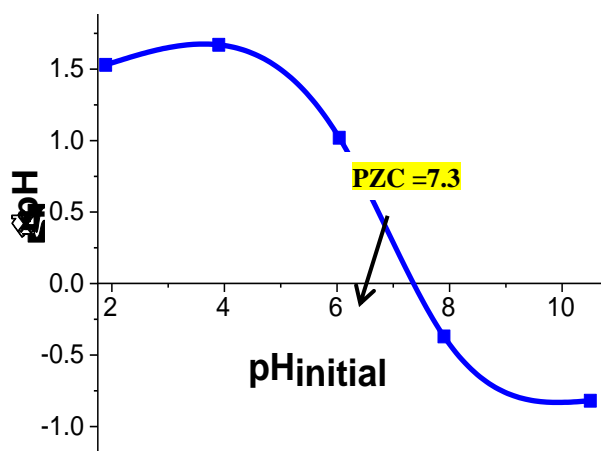


Figure 5: The point of zero charge (pH_{pzc}) for ZnO NPs sample.

3.3 Factors affecting the removal of BPA

3.2.1 Effect of pH

The pH value is a significant factor affecting the sorption process (Bhatnagar, Amit et al., 2010). The removal of BPA was examined over a pH range of 6 –10 as displayed in Figure 6. The result illustrated a strong pH relation with the removed amount of BPA by ZnO NPs. The BPA removal increased with increasing pH, reaching 85.1% at pH 7. Then the BPA removal reduced with further raising pH > 8 where the removal efficiency of BPA declined to 34.7% at pH 10 (Figure 6a). It is known that BPA or phenols are mainly presented in nonionic state at pH range (6 - 7). ZnO NPs gave the maximum BPA uptake at pH =7. The decrease in the removal rate at higher pH >8 may be due to the increased ionization process leading to the increase electrostatic repulsion between BPA and ZnO NPs (PZC = 7.3). When the pH is higher than the BPA's pKa value (9.5–10), the net charge changes to be negative in nature (RaniShanker, 2018). Moreover, Figure 6b shows clearly that the amount of BPA adsorbed (q_e) increased significantly from 0.84 mg/g to 0.92 mg/g by increasing pH from 6 to 9. However, the adsorbed amount decreases dramatically in both acidic and basic pH values. The same trend was observed in other published papers (Orimolade et al., 2018; Wang et al., 2020).

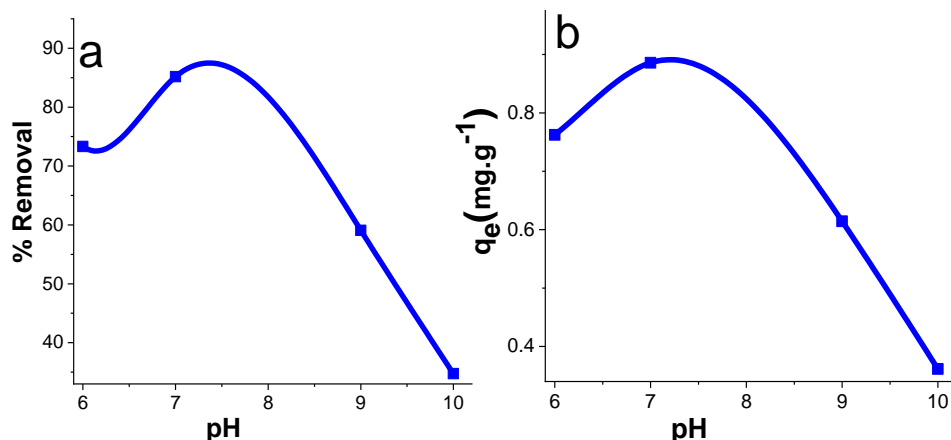


Figure 6: Effect of pH vs. a) % removal b) amount of BPA adsorbed (q_e).

3.2.2 Effect of Initial BPA Concentration

The efficiency of the removal process and the mechanism determining the overall kinetic coefficient are both strongly influenced by the initial concentration of BPA in solution (Krishnan et al., 2017). Figure 7 illustrates the impact of the initial BPA concentration on the BPA removal and the amount of BPA eliminated by ZnO NPs. Hence, lowering the initial BPA concentration showed high efficiency of the removal process (Martín-Lara et al., 2020). By increasing the concentration of BPA from 1 to 5 ppm, the elimination of phenol declined from 84.6% to 57.09%, as illustrated in Figure 7a. This can be explained by the fact that there are too many adsorption sites available to remove BPA at a fixed dosage of ZnO NPs. But, as the initial concentration was increased, more BPA molecules crowded the existing adsorption sites. The same trend was documented by many researchers (RaniShanker, 2018). Also, the amount of BPA adsorbed (q_e) was increased by increasing the concentration of BPA from 1.0 to 5.0 ppm, increasing from 0.88 mg/g to 2.88 mg/g as seen in Figure 7b. This can be explained by how increasing the BPA concentration will enhance the uptake driving force between the ZnO NPs and the BPA (Wang, 2020). Based on the above results, 1ppm as initial BPA concentration was chosen as one optimum condition.

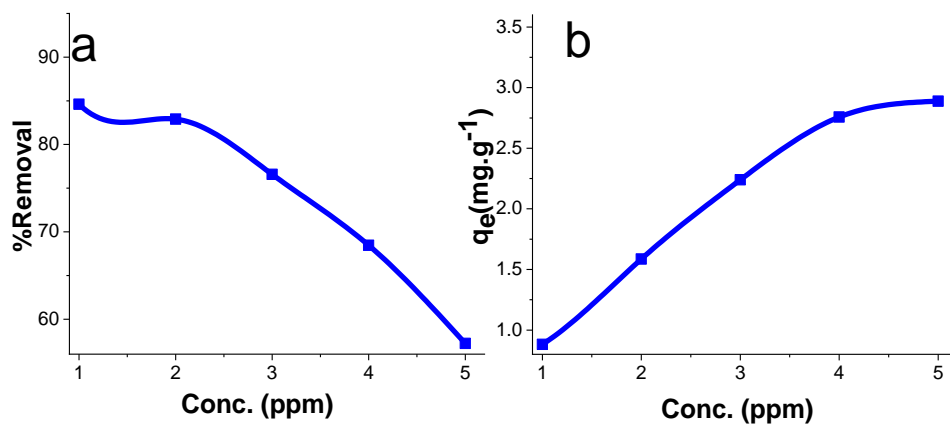


Figure 7: Effect of initial concentration vs. a) % removal b) amount of BPA adsorbed (q_e).

3.2.3 Effect of adsorbent dose on BPA adsorption

It is important to investigate the effects of adsorbent amount (ZnO NPs) on removal system (Balci Erkurt, 2016). As shown in Figure 8a, the removal of BPA increased proportionally with increasing the amount of ZnO NPs. The removal efficiency of BPA increased from 57.8% to 85.1%. This was attributed to the increase in active site with increasing quantity of ZnO NPs. Moreover, at higher ZnO NPs dosages, available surface area may be increased (Martín-Lara et al., 2020; Wang, Y. et al., 2020). The result demonstrated that dosage increases above 1 g L^{-1} had no impact on potential of elimination. Therefore, 1 g L^{-1} of ZnO NPs dosage was chosen for additional experiments. Meanwhile, the amount of BPA adsorbed (q_e) decreased from 6.02 mg/g to 0.44 mg/g , as demonstrated Figure 8b. The quantity (q_e) of removed phenol decreased as these unsaturation adsorption sites multiplied during the removal process since the dose of ZnO NPs was increased. (Lin et al., 2009).

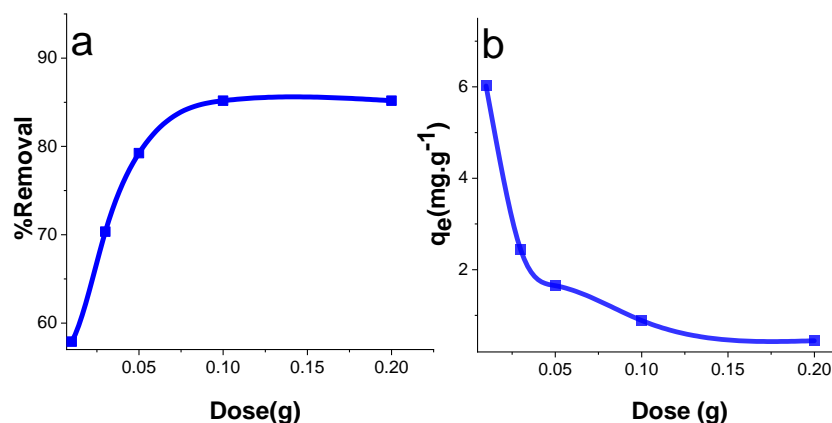


Figure 8: Effect of ZnO NPs dose vs. a) % removal b) amount of BPA adsorbed (q_e).

3.2.4 Effect of contact time on BPA adsorption

Water treatment mainly depends on the contact time that the adsorbate and adsorbent are connected with one another (Krishnan et al., 2017). In fact, the removal of BPA contaminates by the ZnO NPs was a quick with removal efficiency of 64.4% at the first 15 minutes. The BPA elimination by ZnO NPs was strongly affected by contact time. According to this study, the equilibrium time for BPA removal was achieved in 60 minutes with 84.6% removal. After that, a slower step was observed in Figure 9a. The amount q_e of BPA adsorbed onto ZnO NPs also showed the same trend and increased with increasing contact time (Figure 9b). The early stage ZnO surface featured a large number of accessible active sites, which may have enhanced the rapid adsorption process. As the equilibrium was approaching, the sorption reduced in the later stages as these surface sites were gradually filled (Djebri et al., 2020; Katibi et al., 2021; El-Nahas et al., 2020). According to other studies, phenolic compounds had the same impact on graphene oxide (Wang, X. et al., 2018).

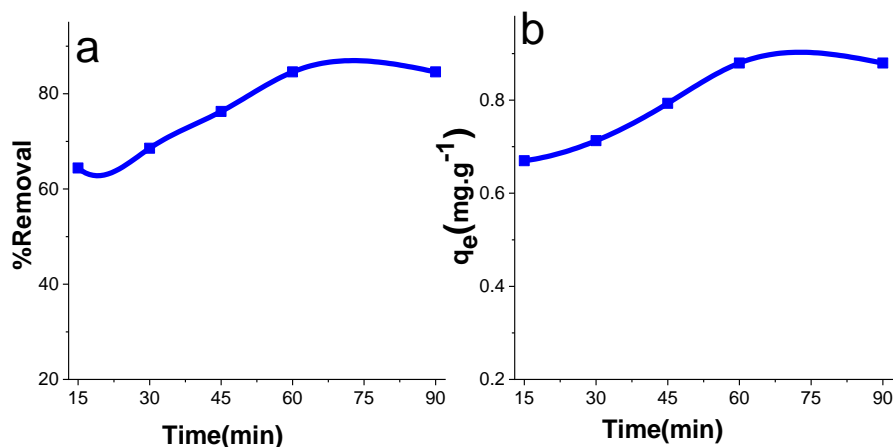


Figure 9: Effect of contact time vs. a) % removal b) amount of BPA adsorbed (q_e).

3.2.5 Influence of temperature on BPA adsorption

The adsorption process is significantly impacted by temperature of solution (Chang et al., 2012). Removal studies of BPA by ZnO NPs were carried out at 25, 35, 45, and 55 °C and the results were displayed in Figure 10 (a, b). Temperature variations can be used to predict whether the removal process would be endothermic or exothermic. Data presented in Figure 10a showed an increase in the removal efficiency of BPA from 81.02 to 88.10% as the temperature increased from 25 to 45 °C, indicating the endothermic process. Also, the amount of BPA adsorbed by ZnO NPs increased from 0.84 mg g⁻¹ to 0.91 mg g⁻¹ (Figure 10b). The outcome of endothermic process can be explained by enhanced molecular interactions between the BPA and the ZnO NPs surface at higher temperature as well as increasing the mobility of BPA molecules with increasing the temperature (Haciosmanoglu et al., 2019; Sun, Z. et al., 2020).

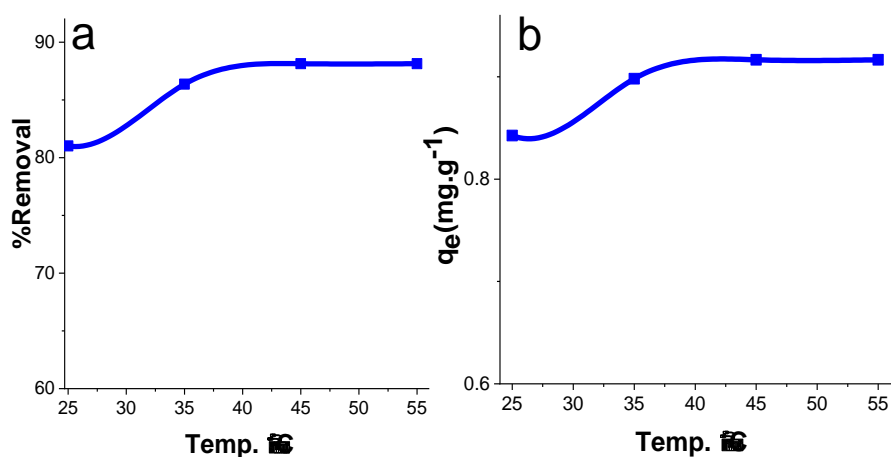


Figure 10: Effect of Temperature vs. a) % removal b) amount of BPA adsorbed (q_e).

3.2.6 Equilibrium Studies

Adsorption isotherms are used to evaluate how the adsorption molecules were distributed between the liquid and solid phases at the equilibrium (Chang et al., 2012). Langmuir, Freundlich, and Temkin isotherms were expressed by equations presented in Table S1. The Langmuir isotherm model supposes monolayer coverage on a homogeneous surface without reaction between adsorbed molecules and uniform energies of adsorption onto the surface (DemiralGunduzoglu, 2010). The maximum adsorption capacity of adsorbent related to monolayer adsorption on the surface of adsorbent can be determined via using this model (Bhatnagar, A.Anastopoulos, 2017; Mazarji et al., 2017). Otherwise, the Freundlich equation is an empirical equation based on adsorption on a heterogeneous energetic distribution of active sites on the surface with interactions between adsorbed molecules. It is not only limited to the creation of the monolayer (DemiralGunduzoglu, 2010; Erhayem et al., 2015). Temkin isotherm model assumes that the fall in the heat of sorption is linear rather than logarithmic. The Temkin model is usually used for heterogeneous surface energy systems, where the heat of adsorption of all the molecules in the layer would decrease linearly with coverage due to adsorbent–adsorbate interactions (Khawar et al., 2019). The linearized Langmuir, Freundlich, and Temkin plots for BPA at fixed temperature (room temp.) are presented in Figure 11. While, their constants and the correlation coefficients were tabulated in Table 3. According to the R^2 values of the three models were 0.99, 0.96, and 0.99 for Langmuir, Freundlich, and Temkin models respectively. These results demonstrated that BPA uptake on the ZnO NPs is complex process and can be explained by a various mechanism (Rahmat et al., 2019). The molecule structure of BPA was like butterfly shape, which gives it a chance to build multilayer adsorption on the heterogeneous area. Additionally, it's possible that the two hydroxyl groups in the BPA molecule will induce the adsorbate to self-assemble by hydrogen bonding, resulting in multilayer adsorption (Phatthanakittiphong Seo, 2016). A favorable adsorption process may be indicated by calculating the adsorption intensity (R_L) value especially when R_L is $0 < R_L < 1$. The variation of the adsorption intensity (R_L) with different initial BPA concentrations C_o (from 1.04 mg L^{-1} to 5.04 mg L^{-1}) is incorporated in Table S2. All the R_L values for BPA adsorption are between 0 and 1, where the range of R_L values was ranged from 0.339 to 0.096. This confirms favorability adsorption process of BPA onto ZnO NPs (Issaoui et al., 2020). Also, the maximum adsorption capacity calculated from Langmuir isotherm equation was found to be 3.8 mg g^{-1} , these values were typically close to those published papers by other authors (Bhatnagar, A.Anastopoulos, 2017; Gomez-Serrano et al., 2021). Furthermore, the high values of the Freundlich isotherm constants (K_f and n) indicated good adsorption process of BPA from aqueous solutions with high adsorptive capacity. The value of Freundlich isotherm constant n is 1.8 ($n > 1$), that indicating good adsorption and surface heterogeneity intensity (Balarak, 2016). Moreover, the high value of K_f (2.6) indicates the high adsorption efficiency for BPA by ZnO NPs. At temperature equals 298K, the value b of Temkin constant ($b = RT/B$) for BPA adsorption onto ZnO NPs was 2.7 KJ/mol showing that adsorbent had the higher affinity for binding with BPA. In conclusion, the adsorption equilibrium of BPA on ZnO NPs described by the Langmuir, Freundlich, and Temkin isotherm models. This indicated that more than one mechanism to explain the adsorption process. Recent critiques focused on employment models in their linear form which can give incorrect values of the fundamental model parameters (El-Nahas, et al., 2021). Figure 12 demonstrates the diagram of nonlinear Langmuir, Freundlich, and Temkin models at 25°C which can be used in explanation the best model for BPA adsorption on ZnO NPs. Also, the findings of nonlinear

forms showed that the process of BPA absorption onto ZnO NPs is multifaceted and that it may be explained by three models.

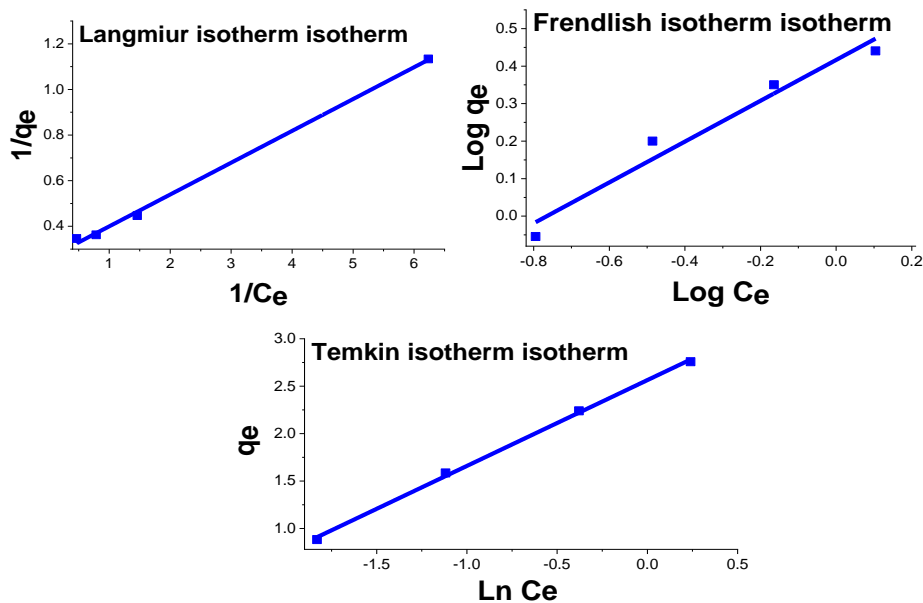


Figure 11: Linear form of a) Langmuir, b) Freundlich and c) Temkin Isotherm of BPA onto ZnO NPs.

Table 3: Langmuir, Freundlich and Temkin Isotherm constant BPA onto ZnO NPs.

Sample	Langmuir constants			Freundlich constant			Temkin constant		
	q_{max} (mg/g)	K_L (mg/L)	R^2	n	K_f (mg/g)	R^2	b KJ/mol	A	R^2
ZnO NPs	3.8	1.86	0.99	1.8	2.6	0.96	2.74	17	0.99

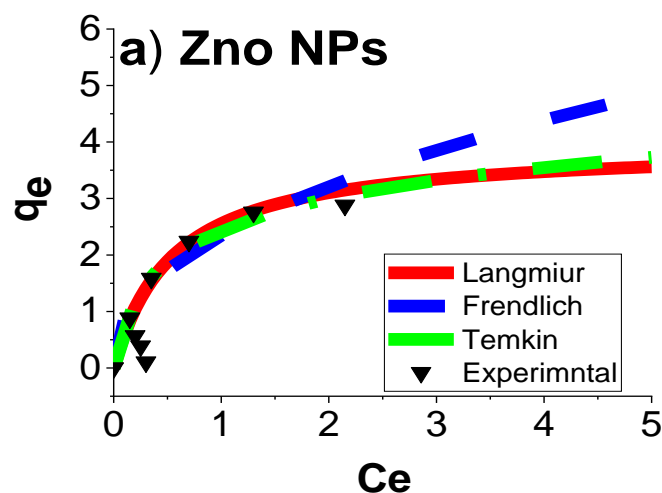


Figure 12: Non-linear form of Freundlich, Langmuir and Temkin Isotherm on adsorption of BPA on ZnO NPs at 25°C.

3.2.7 Kinetic Studies

A kinetic analysis of the adsorption process (the rate of adsorption) can be used to determine the controlling mechanism, which is the crucial factor in mass transfer (Balarak, 2016). Three kinetic models were examined with experimental data for adsorption of BPA by ZnO NPs as a function of time. Pseudo-first-order, pseudo-second-order and intra-particle diffusion were examined as kinetic models. The equations in Table 3 mainly illustrates the kinetics parameter for the three models. Figure 13 displayed the plots of kinetic BPA adsorption onto the ZnO NPs samples. According to the data presented in Table 4, it showed higher linearity to the pseudo-second order model than the pseudo-first order model. Where the correlation coefficients (R^2) for the pseudo-second order model ($R^2 = 0.99$) was higher value than (R^2) for the pseudo-first order equation (0.69). Additionally, the theoretical q_e values derived from the pseudo-second equation were closed to those of experimental q_e values (El Kady et al., 2016). It's important to noted that pseudo-second-order kinetics don't completely describe just only the chemisorption process. Pseudo-second order models can also be used to explain also the ion exchange process at charged surfaces (El-Nahas et al., 2020). Besides, Figure 13 illustrated intraparticle diffusion model (q_t vs. $t^{0.5}$ plot) which exhibited three independent linear portions, and the plot's intercept did not pass through its origin. This would suggest that the adsorption process involves more than one kinetic stage that the removal of BPA onto ZnO NPs sample is complex and the intraparticle diffusion is not the only rate-limiting step for the whole reaction (El-Nahas et al., 2018)

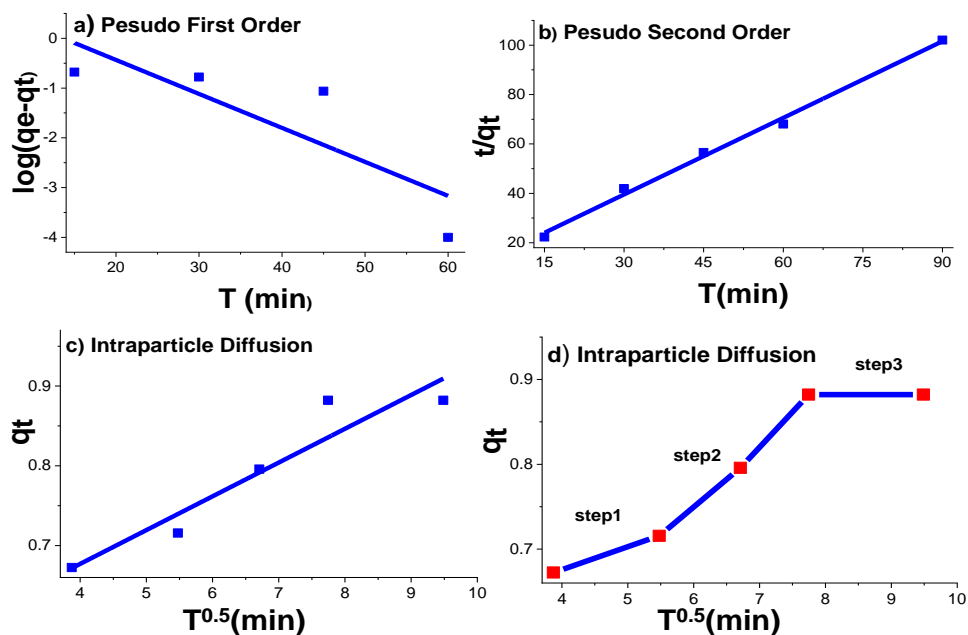


Figure 13: Kinetic Studies: a) pseudo-first, b) pseudo second and c) intra diffusion of BPA onto ZnO NPs.

Table 4: Kinetic Studies, pseudo-first, pseudo second and intraparticle diffusion Constant of BPA onto ZnO NPs.

Sample	Pseudo-first order			Pseudo-second order			Intraparticle diffusion		q_e (Exp)
	K_1	q_e	R^2	K_2	q_e	R^2	K_{ad}	R_2	
ZnO NPs	0.157	8.56	0.69	0.109	0.96	0.99	0.042	0.90	0.88

3.2.8 Thermodynamic parameters

Thermodynamic parameters are crucial in the design of any reactor since they may help in increasing the efficiency and predict the type of the adsorption process. Adsorption parameters are produced using two types of thermodynamic properties (Tamjidi et al., 2021). Thermodynamic constants like Gibbs free energy (ΔG°), enthalpy (ΔH°), and entropy (ΔS°) are used to identify the nature of the sorption process. Equations in Table 4 demonstrated the thermodynamic parameters for adsorption process. As seen in Figure S1 and data presented in Table 5, thermodynamic constants were described by Van't Hoff equation. The data showed the negative values of (ΔG°), indicating reaction takes place spontaneously across the entire temperature range. The ΔG° values were more negatively by increasing temperature suggesting that the removal process was more favorable at higher temperatures. Besides, ΔH° and ΔS° have the same algebraic sign that confirms the sorption processes are favored at higher temperatures. A positive ΔS° value for entropy shows that BPA has an affinity for the ZnO NPs adsorbent at high temperature (De Farias et al., 2022; Mphahlele et al., 2015). Furthermore, a positive values

of ΔH° were observed indicating the endothermic nature of adsorption besides significant interaction between the adsorbate and adsorbents via multiple mechanisms (adsorption and/or complexation) (Argani et al., 2018; Kim et al., 2020).

Table 5: Thermodynamic constants for sorption system of BPA onto ZnO NPs sample.

Sample	ΔH° (kJ/mol)	ΔS° (kJ/mol)	ΔG° (kJ/mol)			
			25 °C	35 °C	45 °C	55 °C
ZnO NPs	15	0.630	-3.83	-4.78	-5.41	-6.04

3.3 Mechanism for removal

The removal of BPA can take place via various possible mechanisms. Factors that affect the preference of the adsorption may be related to the characteristics of the binding sites (e.g. functional groups, structure, surface properties, etc.), the properties of the adsorbate (e.g. concentration, ionic size, ionic charge, molecular structure etc.), and the solution chemistry (e.g. pH, ionic strength, temperature, etc.). The functional groups (OH groups) in BPA are mainly the responsible for the binding abilities with the surface of the ZnO NPs. In acidic environments, both BPA's hydroxyl groups and surfaces of ZnO NPs can be protonated, creating positive charges causing electrostatic repulsion with each other. That explains why BPA can only be removed to a limited extent in acidic media. ZnO NP's oxygen groups play a significant role in its capacity to bind BPA. The creation of hydrogen bonds between the hydroxyl groups of BPA and the surface oxygen of ZnO NPs is the basis for the adsorptive removal of BPA (Allam et al., 2021). In contrast, the surface of ZnO NPs becomes negatively charged in alkaline conditions (PZC > 7.3), as demonstrated in Figure 14. Furthermore, BPA's pKa value is between (9.5 and 10) and produces the ionic species BPA^{2-} and BPA^- , which increases electrostatic repulsion and makes BPA removal difficult in basic medium (Katibi et al., 2021).

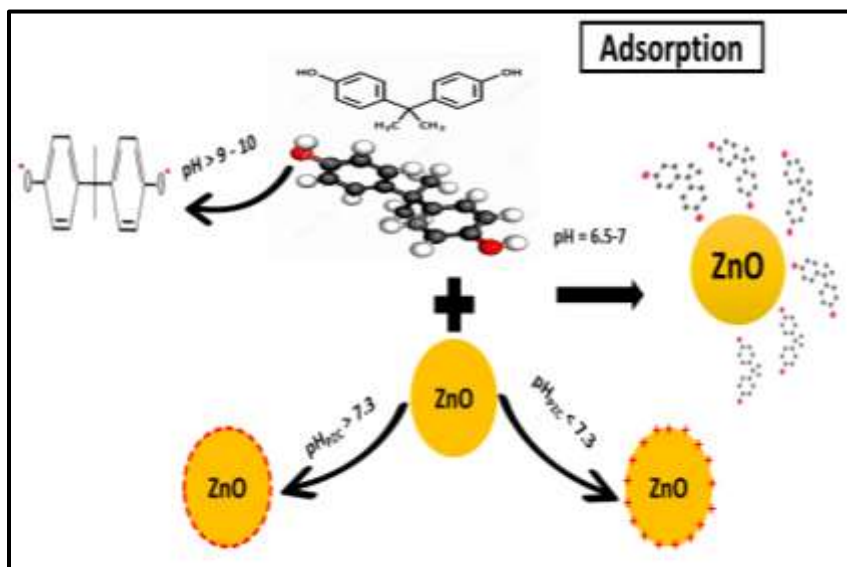


Figure 14: Schematic representation of the mechanism for removal of BPA onto ZnO NPs.

4. Comparative Study with previous studies

The uptake capacity of BPA by several materials compared with ZnO NPs in this study are shown in Table 6. The ZnO NPs employed in this research has good ability for elimination of amounts of BPA from water sources exceed 85% removal.

Table 6: Comparison between tested ZnO NPs material with other published materials for removal BPA

Materials	Dosage of adsorbent	Initial conditions (ppm)	%Removal efficiency	Ref
neat biochar (NBC)	2 g/L	20 ppm	48.45%	(Katibi et al., 2021)
magnetic biochar	2 g/L	20 ppm	60.0%	
banana fronds	9 g/L	20 ppm	59.97%	(Rahmat et al., 2019)
Commercial chitosan	0.06 g/L	0.1 ppm	58%	(Dehghani et al., 2016)
Synthesized chitosan	0.06 g/L	0.1 ppm	78%	
ZnO NPs	1 g/L	1 ppm	85%	This study

5. CONCLUSION

The main goal of this search was to study the adsorptive removal of organic contaminants bisphenol-A (BPA) onto ZnO NPs to purify water sources. The ZnO NPs were synthesis by aiding the microwave irradiation and gave rod like shape. The equilibrium results were successfully fitted well with both Langmuir isotherm model and Temkin isotherm model. Furthermore, the BPA removal followed well with pseudo-second-order kinetics. The removal process had a positive ΔH° value indication the endothermic nature. All the above results indicated that more than mechanism was involved for removal of BPA onto ZnO NPs surface. The best operating factors for removal of BPA from water were obtained at pH 7, contact time 60 min. A good adsorptive capacity of BPA was achieved to be 85%.

6. RECOMMENDATION

- ✓ We suggest adding small amount of zinc oxide to the kaolin paste to improve the ceramic properties that help for BPA removal.
- ✓ Water should be stored in non-plastic containers to prevent the release of harmful compounds like bisphenol A or the need for adsorbents to remove these contaminants.

References

- Abd Mutalib, M., Rahman, M.A., Othman, M.H.D., Ismail, A.F. and Jaafar, J. 2017. "Scanning Electron Microscopy (SEM) and Energy-Dispersive X-Ray (EDX) Spectroscopy". In *Membrane Characterization* pp. 161-179.
- Allam, E.A., Ali, A.S.M., Elsharkawy, R.M. and Mahmoud, M.E. 2021. "Framework of nano metal oxides N-NiO@N-Fe₃O₄@N-ZnO for adsorptive removal of atrazine and bisphenol-A from wastewater: Kinetic and adsorption studies". *Environmental Nanotechnology, Monitoring & Management*, 16. doi:10.1016/j.enmm.2021.100481.
- Argani, H., Latifa Bouamrani, M., Yousfi, S., Hamed El-Kouali, M., Talbi, M. and Atmani, R. 2018. "Adsorption Process of Cu(II) Cations by Using the Waste of Phosphate Rock (WPR) as Novel Adsorbent material". *Oriental Journal of Chemistry*, 344, 1908-1918. doi:10.13005/ojc/3404026.

- Balarak, D. 2016. "Kinetics, Isotherm and Thermodynamics Studies on Bisphenol A Adsorption using Barley husk". *International Journal of ChemTech Research*. International Journal of ChemTech Research, 9, 2455-9555
- Balci, B. and Erkurt, F.E. 2016. "Adsorption of Bisphenol-A by Eucalyptus bark/magnetite composite: Modeling the effect of some independent parameters by multiple linear regression". *Adsorption Science & Technology*, 353-4, 339-356. doi:10.1177/02636174166676819.
- Barzegari, Z., Bina, B., Pourzamani, H.R. and Ebrahimi, A. 2015. "The combined treatment of bisphenol A (BPA) by coagulation/flocculation (C/F) process and UV irradiation in aqueous solutions". *Desalination and Water Treatment*, 5719, pp :8802-8808. doi:10.1080/19443994.2015.1030706.
- Bezzon, V.D.N., Pinto, R.D.S., De Araujo, G.L.B., De Lima, J.C. and Ferreira, F.F. 2022. "Describing the Influence of Ball-milling on the Amorphization of Flubendazole Using the PDF and RMC Methods with X-ray Powder Diffraction Data". *J Pharm Sci*. doi:10.1016/j.xphs.2022.06.018.
- Bhatnagar, A. and Anastopoulos, I. 2017. "Adsorptive removal of bisphenol A (BPA) from aqueous solution: A review". *Chemosphere*, 168, 885-902. doi:10.1016/j.chemosphere.2016.10.121.
- Bhatnagar, A., Kumar, E. and Sillanpää, M. 2010. "Nitrate removal from water by nano-alumina: Characterization and sorption studies". *Chemical Engineering Journal*, 1633, 317-323. doi:10.1016/j.cej.2010.08.008.
- Chang, K.-L., Hsieh, J.-F., Ou, B.-M., Chang, M.-H., Hsieh, W.-Y., Lin, J.-H., Huang, P.-J., Wong, K.-F. and Chen, S.-T. 2012. "Adsorption Studies on the Removal of an Endocrine-Disrupting Compound (Bisphenol A) using Activated Carbon from Rice Straw Agricultural Waste". *Separation Science and Technology*, 4710, 1514-1521. doi:10.1080/01496395.2011.647212.
- Davoud Balarak, F.K.M., Seung Mok Lee, and Choong Jeon. June 2019. "Adsorption of Bisphenol A Using Dried Rice Husk: Equilibrium, Kinetic and Thermodynamic Studies". 30. doi:10.14478/ace.2019.1013.
- De Farias, M.B., Silva, M.G.C. and Vieira, M.G.A. 2022. "Adsorption of bisphenol A from aqueous solution onto organoclay: Experimental design, kinetic, equilibrium and thermodynamic study". *Powder Technology*, 395, 695-707. doi:10.1016/j.powtec.2021.10.021.
- Dehghani, M.H., Ghadermazi, M., Bhatnagar, A., Sadighara, P., Jahed-Khaniki, G., Heibati, B. and McKay, G. 2016. "Adsorptive removal of endocrine disrupting bisphenol A from aqueous solution using chitosan". *Journal of Environmental Chemical Engineering*, 43, 2647-2655. doi:10.1016/j.jece.2016.05.011.
- Demiral, H. and Gunduzoglu, G. 2010. "Removal of nitrate from aqueous solutions by activated carbon prepared from sugar beet bagasse". *Bioresour Technol*, 1016, 1675-1680. doi:10.1016/j.biortech.2009.09.087.
- Divband Hafshejani, L., Hooshmand, A., Naseri, A.A., Mohammadi, A.S., Abbasi, F. and Bhatnagar, A. 2016. "Removal of nitrate from aqueous solution by modified sugarcane bagasse biochar". *Ecological Engineering*, 95, 101-111. doi:10.1016/j.ecoleng.2016.06.035.

- Djebri, N., Noufel, K., Boukhalfa, N., Sid, D. and Boutahala, M. 2020. "Single and binary component adsorption of endocrine disrupting chemicals from aqueous solutions using calcium alginate/apricot stone-activated carbon composite bead". *Desalination and Water Treatment*, 197, 170-181. doi:10.5004/dwt.2020.25911.
- Baird, R. B., Eaton, A. D., & Clesceri, L. S. (2017). Standard methods for the examination of water and wastewater (Vol. 10). E. W. Rice (Ed.). Washington, DC: American public health association part 5530 D. (Direct Photometric Method)
- El-Nahas, S., El-Sadek, M.S.A., Salman, H.M. and Elkady, M.M. 2021. "Controlled morphological and physical properties of ZnO nanostructures synthesized by domestic microwave route". *Materials Chemistry and Physics*, 258. doi:10.1016/j.matchemphys.2020.123885.
- El-Nahas, S., Osman, A.I., Arafat, A.S., Al-Muhtaseb, A.a.H. and Salman, H.M. 2020. "Facile and affordable synthetic route of nano powder zeolite and its application in fast softening of water hardness". *Journal of Water Process Engineering*, 33. doi:10.1016/j.jwpe.2019.101104.
- El-Nahas, S., Salman, H. and Seleem, W. 2017. "A New and Successful Utilization of Egyptalum Company Solid Waste in Adsorptive Removal of Nitrates from Water Supplies". *International Research Journal of Pure and Applied Chemistry*, 153, 1-17. doi:10.9734/irjpac/2017/38221.
- El-Nahas, S., Salman, H.M. and Saber, A.M. 2021. "Production of low-price carbon for removal of aluminium ions in potable water". *Journal of Environmental Engineering and Science*, 163, 145-164. doi:10.1680/jenes.20.00055.
- El-Nahas, S., Salman, H.M. and Seleem, W.A. 2018. "Aluminum Building Scrap Wire, Take-Out Food Container, Potato Peels and Bagasse as Valueless Waste Materials for Nitrate Removal from Water supplies". *Chemistry Africa*, 21, 143-162. doi:10.1007/s42250-018-00032-z.
- El Kady, M., Shokry, H. and Hamad, H. 2016. "Effect of superparamagnetic nanoparticles on the physicochemical properties of nano hydroxyapatite for groundwater treatment: adsorption mechanism of Fe(ii) and Mn(ii)". *RSC Advances*, 685, 82244-82259. doi:10.1039/c6ra14497g.
- Elobeid, M.A., Almarhoon, Z.M., Virk, P., Hassan, Z.K., Omer, S.A., Elamin, M., Daghestani, M.H. and Alolayan, E.M. 2012. "Bisphenol A Detection in Various Brands of Drinking Bottled Water in Riyadh, Saudi Arabia Using Gas Chromatography/Mass Spectrometer". *Tropical Journal of Pharmaceutical Research*, 113. doi:10.4314/tjpr.v11i3.15.
- Englande Jr, A. J., Krenkel, P., & Shamas, J. (2015). *Wastewater treatment & water reclamation. Reference module in earth systems and environmental sciences.*
- Erhayem, M., Al-Tohami, F., Mohamed, R. and Ahmida, K. 2015. "Isotherm, Kinetic and Thermodynamic Studies for the Sorption of Mercury (II) onto Activated Carbon from *Rosmarinus officinalis* Leaves". *American Journal of Analytical Chemistry*, 0601, 1-10. doi:10.4236/ajac.2015.61001.
- Evode, N., Qamar, S.A., Bilal, M., Barceló, D. and Iqbal, H.M.N. 2021. "Plastic waste and its management strategies for environmental sustainability". *Case Studies in Chemical and Environmental Engineering*, 4. doi:10.1016/j.cscee.2021.100142.

- Godwin, J., Abdus-Salam, N., Panda, P.K. and Tripathy, B.C. 2022. "Special Crystal Growth and Nucleation process of Zinc Oxide Nanoparticles from Urea Solution for E". doi:10.21203/rs.3.rs-1625280/v1.
- Gomez-Serrano, V., Adame-Pereira, M., Alexandre-Franco, M. and Fernandez-Gonzalez, C. 2021. "Adsorption of bisphenol A by activated carbon developed from PET waste by KOH activation". *Environ Sci Pollut Res Int*, 2819, 24342-24354. doi:10.1007/s11356-020-08428-6.
- Haciosmanoglu, G.G., Dogruel, T., Genc, S., Oner, E.T. and Can, Z.S. 2019. "Adsorptive removal of bisphenol A from aqueous solutions using phosphonated levan". *J Hazard Mater*, 374, 43-49. doi:10.1016/j.jhazmat.2019.04.015.
- Hasanpoor, M., Aliofkhaezrai, M. and Delavari, H. 2015. "Microwave-assisted Synthesis of Zinc Oxide Nanoparticles". *Procedia Materials Science*, 11, 320-325. doi:10.1016/j.mspro.2015.11.101.
- Hoekstra, E.J. and Simoneau, C. 2013. "Release of bisphenol A from polycarbonate: a review". *Crit Rev Food Sci Nutr*, 534, 386-402. doi:10.1080/10408398.2010.536919.
- Issaoui, O., Amor, H.B., Ismail, M., Pirault-Roy, L. and Jeday, M.R. 2020. "Adsorption of Bisphenol A from Aqueous Solution by HDTMA-Tunisian Clay Synthesized Under Microwave Irradiation: A Parametric and Thermodynamic Study". *Clays and Clay Minerals*, 684, 361-372. doi:10.1007/s42860-020-00079-5.
- Zhang, J., Sun, L., Yin, J., Su, H., Liao, C., & Yan, C. (2002). Control of ZnO morphology via a simple solution route. *Chemistry of Materials*, 14(10), 4172-4177.
- Kang, J.H., Kondo, F. and Katayama, Y. 2006. "Human exposure to bisphenol A". *Toxicology*, 2262-3, 79-89. doi:10.1016/j.tox.2006.06.009.
- Katibi, K.K., Yunos, K.F., Man, H.C., Aris, A.Z., Mohd Nor, M.Z. and Azis, R.S. 2021. "An Insight into a Sustainable Removal of Bisphenol A from Aqueous Solution by Novel Palm Kernel Shell Magnetically Induced Biochar: Synthesis, Characterization, Kinetic, and Thermodynamic Studies". *Polymers (Basel)*, 1321. doi:10.3390/polym13213781.
- Khawar, A., Aslam, Z., Zahir, A., Akbar, I. and Abbas, A. 2019. "Synthesis of Femur extracted hydroxyapatite reinforced nanocomposite and its application for Pb(II) ions abatement from aqueous phase". *Int J Biol Macromol*, 122, 667-676. doi:10.1016/j.ijbiomac.2018.10.223.
- Kim, M., Choong, C.E., Hyun, S., Park, C.M. and Lee, G. 2020. "Mechanism of simultaneous removal of aluminum and fluoride from aqueous solution by La/Mg/Si-activated carbon". *Chemosphere*, 253, 126580. doi:10.1016/j.chemosphere.2020.126580.
- Koduru, J.R., Lingamdinne, L.P., Singh, J. and Choo, K.-H. 2016. "Effective removal of bisphenol A (BPA) from water using a goethite/activated carbon composite". *Process Safety and Environmental Protection*, 103, 87-96. doi:10.1016/j.psep.2016.06.038.
- Krishnan G, R., Radhika, R., Jayalatha, T., Jacob, S., Rajeev, R., K. George, B. and Anjali, B.R. 2017. "Removal of perchlorate from drinking water using granular activated carbon modified by acidic functional group: Adsorption kinetics and equilibrium studies". *Process Safety and Environmental Protection*, 109, 158-171. doi:10.1016/j.psep.2017.03.014.
- Lin, K., Pan, J., Chen, Y., Cheng, R. and Xu, X. 2009. "Study the adsorption of phenol from aqueous solution on hydroxyapatite nanopowders". *J Hazard Mater*, 1611, 231-240. doi:10.1016/j.jhazmat.2008.03.076.

- Mainali, K. 2020. "Phenolic Compounds Contaminants in Water: A Glance". *Current Trends in Civil & Structural Engineering*, 44. doi:10.33552/ctcse.2020.04.000593.
- Manisalidis, I., Stavropoulou, E., Stavropoulos, A. and Bezirtzoglou, E. 2020. "Environmental and Health Impacts of Air Pollution: A Review". *Front Public Health*, 8, 14. doi:10.3389/fpubh.2020.00014.
- Martín-Lara, M.A., Calero, M., Ronda, A., Iáñez-Rodríguez, I. and Escudero, C. 2020. "Adsorptive Behavior of an Activated Carbon for Bisphenol A Removal in Single and Binary (Bisphenol A—Heavy Metal) Solutions". *Water*, 128. doi:10.3390/w12082150.
- Mazarji, M., Aminzadeh, B., Baghdadi, M. and Bhatnagar, A. 2017. "Removal of nitrate from aqueous solution using modified granular activated carbon". *Journal of Molecular Liquids*, 233, 139-148. doi:10.1016/j.molliq.2017.03.004.
- Gaba, M., & Dhingra, N. (2011). Microwave chemistry: General features and applications. *Ind J Pharm Edu Res*, 45(2), 175-183.
- Mphahlele, K., Onyango, M.S. and Mhlanga, S.D. 2015. "Kinetics, Equilibrium, and Thermodynamics of the Sorption of Bisphenol A onto N-CNTs-β-Cyclodextrin and Fe/N-CNTs-β-Cyclodextrin Nanocomposites". *Journal of Nanomaterials*, 2015, 1-13. doi:10.1155/2015/214327.
- Orimolade, B.O., Adekola, F.A. and Adebayo, G.B. 2018. "Adsorptive removal of bisphenol A using synthesized magnetite nanoparticles". *Applied Water Science*, 81. doi:10.1007/s13201-018-0685-y.
- Park, J. and Regalbuto, J.R. 1995. "A Simple, Accurate Determination of Oxide PZC and the Strong Buffering Effect of Oxide Surfaces at Incipient Wetness". *Journal of Colloid and Interface Science*, 1751, 239-252. doi:10.1006/jcis.1995.1452.
- Phatthanakittiphong, T. and Seo, G.T. 2016. "Characteristic Evaluation of Graphene Oxide for Bisphenol A Adsorption in Aqueous Solution". *Nanomaterials (Basel)*, 67. doi:10.3390/nano6070128.
- Rahmat, N.A., Hadibarata, T., Yuniarto, A., Elshikh, M.S. and Syafiuddin, A. 2019. "Isotherm and kinetics studies for the adsorption of bisphenol A from aqueous solution by activated carbon of *Musa acuminata*". *IOP Conference Series: Materials Science and Engineering*, 495. doi:10.1088/1757-899x/495/1/012059.
- Rani, M. and Shanker, U. 2018. "Insight in to the degradation of bisphenol A by doped ZnO@ZnHCF nanocubes: High photocatalytic performance". *J Colloid Interface Sci*, 530, 16-28. doi:10.1016/j.jcis.2018.06.070.
- Rezaeizadeh, M., Hajiabadi, S.H., Aghaei, H. and Blunt, M.J. 2021. "Pore-scale analysis of formation damage; A review of existing digital and analytical approaches". *Adv Colloid Interface Sci*, 288, 102345. doi:10.1016/j.jcis.2020.102345.
- Rubin, B.S. 2011. "Bisphenol A: an endocrine disruptor with widespread exposure and multiple effects". *J Steroid Biochem Mol Biol*, 1271-2, 27-34. doi:10.1016/j.jsbmb.2011.05.002.
- Scimeca, M., Bischetti, S., Lamsira, H.K., Bonfiglio, R. and Bonanno, E. 2018. "Energy Dispersive X-ray (EDX) microanalysis: A powerful tool in biomedical research and diagnosis". *Eur J Histochem*, 621, 2841. doi:10.4081/ejh.2018.2841.
- Sheikh, M., Pazirofteh, M., Dehghani, M., Asghari, M., Rezakazemi, M., Valderrama, C. and Cortina, J.L. 2020. "Application of ZnO nanostructures in ceramic and polymeric membranes

- for water and wastewater technologies: A review". *Chemical Engineering Journal*, 391. doi:10.1016/j.cej.2019.123475.
- Siddiqi, K.S., Ur Rahman, A., Tajuddin and Husen, A. 2018. "Properties of Zinc Oxide Nanoparticles and Their Activity Against Microbes". *Nanoscale Res Lett*, 131, 141. doi:10.1186/s11671-018-2532-3.
- Singh, D.K., Pandey, D.K., Yadav, R.R. and Singh, D. 2012. "A study of nanosized zinc oxide and its nanofluid". *Pramana*, 785, 759-766. doi:10.1007/s12043-012-0275-8.
- Soliman, M.M.A., Karmakar, A., Alegria, E.C.B.A., Ribeir, A.P.C., Rúbio, G.M.D.M., Saraiva, M.S., Da Silva, M.F.C.G. and Pombeiro, A.J.L. 2020. "ZnO nanoparticles: An efficient catalyst for transesterification reaction of α -keto carboxylic esters". *Catalysis Today*, 348, 72-79. doi:10.1016/j.cattod.2019.08.053.
- Sun, R., Wang, Y., Ni, Y. and Kokot, S. 2014. "Spectrophotometric analysis of phenols, which involves a hemin-graphene hybrid nanoparticles with peroxidase-like activity". *J Hazard Mater*, 266, 60-67. doi:10.1016/j.jhazmat.2013.12.006.
- Sun, Z., Zhao, L., Liu, C., Zhen, Y. and Ma, J. 2020. "Fast adsorption of BPA with high capacity based on π - π electron donor-acceptor and hydrophobicity mechanism using an in-situ sp^2 C dominant N-doped carbon". *Chemical Engineering Journal*, 381. doi:10.1016/j.cej.2019.122510.
- Tamjidi, S., Moghadas, B.K., Esmaili, H., Shakerian Khoo, F., Gholami, G. and Ghasemi, M. 2021. "Improving the surface properties of adsorbents by surfactants and their role in the removal of toxic metals from wastewater: A review study". *Process Safety and Environmental Protection*, 148, 775-795. doi:10.1016/j.psep.2021.02.003.
- Wang, J. and Zhang, M. 2020. "Adsorption Characteristics and Mechanism of Bisphenol A by Magnetic Biochar". *Int J Environ Res Public Health*, 173. doi:10.3390/ijerph17031075.
- Wang, X., Chen, A., Chen, B. and Wang, L. 2020. "Adsorption of phenol and bisphenol A on river sediments: Effects of particle size, humic acid, pH and temperature". *Ecotoxicol Environ Saf*, 204, 111093. doi:10.1016/j.ecoenv.2020.111093.
- Wang, X., Hu, Y., Min, J., Li, S., Deng, X., Yuan, S. and Zuo, X. 2018. "Adsorption Characteristics of Phenolic Compounds on Graphene Oxide and Reduced Graphene Oxide: A Batch Experiment Combined Theory Calculation". *Applied Sciences*, 810. doi:10.3390/app8101950.
- Wang, Y., Hu, K., Yang, Z., Ye, C., Li, X. and Yan, K. 2020. "Facile Synthesis of Porous ZnO Nanoparticles Efficient for Photocatalytic Degradation of Biomass-Derived Bisphenol A Under Simulated Sunlight Irradiation". *Front Bioeng Biotechnol*, 8, 616780. doi:10.3389/fbioe.2020.616780.
- Yıldırım, Ö.A. and Durucan, C. 2010. "Synthesis of zinc oxide nanoparticles elaborated by microemulsion method". *Journal of Alloys and Compounds*, 5062, 944-949. doi:10.1016/j.jallcom.2010.07.125.
- Baird B. Rodger, Rice W.E., and Eaton D. Andrew (2017). Standard Methods for the Examination of Water and Wastewater. In *Standard Methods For The Examination Of Water And Wastewater 23th*: Amer Public Health